

# Oxidative Scrubber for NO<sub>x</sub> Emission Control Using NaClO<sub>2</sub> Aqueous Solutions

Domenico Flagiello\*, Francesco Di Natale, Alessandro Erto, Amedeo Lancia

Department of Chemical, Materials and Production Engineering, University of Naples Federico II, P.le Tecchio, 80 - 80125 Naples, Italy  
[domenico.flagiello@unina.it](mailto:domenico.flagiello@unina.it)

Oxidative scrubbing using different oxidizing chemicals (e.g. sodium chlorite, NaClO<sub>2</sub>) has been proposed since several years for gas emissions control. Although higher performances than conventional after-treatment process currently in use can be reached, these technologies have not yet found a consolidated application in the power generation and other industrial fields, due to excessive chemical consumption and the formation of some harmful contaminants in the wash water that must be removed with specific treatment systems.

This work reports an experimental investigation of an oxidative wet scrubber for NO<sub>x</sub> removal from a simulated flue-gas containing 1030 ppm<sub>v</sub> of nitrogen oxides, using a scrubbing liquid doped with sodium chlorite (NaClO<sub>2</sub>) as oxidizing chemical. The experiments are performed in a packed column operating in counter-current flow with a constant gas velocity of 1.15 m/s at 60 °C and a liquid-to-gas ratio variable from 1.25 to 4.06 L/m<sup>3</sup>. The packed column with a DN 100 is equipped with 892 mm of Mellapak 250.X packing.

The experimental removal efficiencies of NO<sub>x</sub> are evaluated in function of the liquid flow rate and NaClO<sub>2</sub> loading. These data allow to determine the specific NaClO<sub>2</sub> dosage required to achieve a fixed NO<sub>x</sub> removal. Finally, a predictive correlation for wet oxidative scrubbing is also developed.

## 1. Introduction

Nowadays, the NO<sub>x</sub> emission control from flue-gases is still one of the major issues in the fields of energy generation, municipal waste incineration, internal combustion engines and industrial combustion processes. After-treatment de-NO<sub>x</sub> systems are the only option for existing plants and, despite the significant efforts made to improve design and operation of combustion systems aimed to reduce the NO<sub>x</sub> emissions in the flue-gases, they still remain a main option also for new installations. The Selective Catalytic Reduction (SCR) or thermal Selective Non-Catalytic Reduction (SNCR) units are the most used technologies for NO<sub>x</sub> emission control (Muzio et al., 2002; Van Caneghem et al., 2016). SCR is probably the most adopted after-treatment process and has been the subject of several technical and scientific studies aimed to improve conventional units and solve the typical drawbacks on catalyst operational, such as sintering due to high operating temperatures, sulphur and metal poisoning, catalysis competition effects and catalyst longevity (Gao et al., 2017). In spite of the improvements, these units suffer for the high capital investments (CAPEX) and operation and maintenance (O&M) costs, and when the flue-gas is cold or contains large amount of aerosols. In addition, their integration with desulphurization wet scrubbers, needed to assure a fair reduction of SO<sub>x</sub> compounds, is still not straightforward. In this paper, we propose a NO<sub>x</sub> removal system based on a wet oxidative scrubbing process using a chemical oxidant dissolved in aqueous solutions (Brogren et al., 1998). This technology potentially offers simpler and lighter equipment than SCR units, also determining much lower installation costs, if the oxidant consumption is optimized with a scrubber recirculation system and a specific water treatment plant is installed after scrubbing. In addition, the low operating temperature makes this unit very suitable as an end-of-pipe process for retrofitting of existing SCR/SNCRs when further NO<sub>x</sub> reductions are mandatory. This allows to comply with the more stringent regulations recently set at European level (Directive (EU) 2016/2284), which require a reduction of NO<sub>x</sub> emissions of about 35 - 40% by 2030 and 60 - 70% after 2030. In this work, we report preliminary findings on NO<sub>x</sub> emission control by an oxidative scrubbing. In details, the oxidative scrubber operates with sodium chlorite (NaClO<sub>2</sub>), which is a very strong chemical oxidant

when dissolved in aqueous solutions. The experiments were performed in a pilot-scale scrubber having a diameter of 0.1 m and a height of 0.892 m, filled with Mellapak 250.X structured packing. The tests were performed with a simulated flue-gas stream with a constant gas flow rate of 32 m<sup>3</sup>/h containing 1030 ppm<sub>v</sub> of NO<sub>x</sub> at 60 °C (typical value of the end-of-pipe processes). The scrubbing solutions was an aqueous solution containing a concentration of NaClO<sub>2</sub> ranging from 0 to 1% w/w, fed with liquid to gas ratios between 1.25 - 4.06 L/m<sup>3</sup>.

## 2. Absorption mechanism of NO<sub>x</sub> in NaClO<sub>2</sub> aqueous solutions

NO<sub>(g)</sub> is a gas almost insoluble in water and it accounts for more than 90% of NO<sub>x</sub> in a typical flue-gas, where the rest is mainly NO<sub>2(g)</sub>. NO<sub>x</sub> absorption from a gaseous stream in water is characterized by a complex network of reactions, involving many compounds in both gas and liquid phase, and their interactions make this process much complicated (Hoftyzer and Kwanten, 1972). Indeed, there are many parallel and series reactions together with absorption and desorption phenomena of the species in solution, simultaneously (Figure 1).

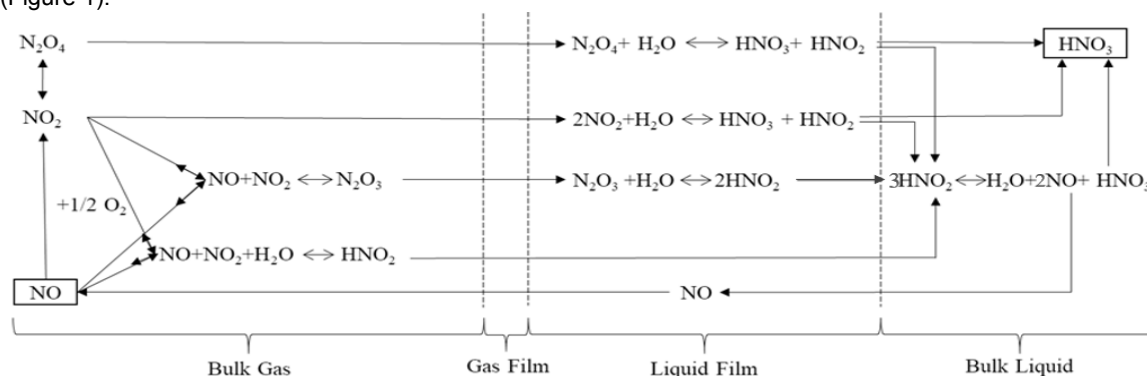


Figure 1: Reactive scheme for NO<sub>x</sub> absorption in water (Hoftyzer and Kwanten (1972))

NO<sub>(g)</sub> absorption is mainly related to both NO<sub>2(g)</sub> formation, which is about one order of magnitude more soluble in water than NO, and also N<sub>2</sub>O<sub>4(g)</sub> and N<sub>2</sub>O<sub>3(g)</sub> formation, both much more soluble in water than nitrogen dioxide (Hoftyzer and Kwanten, 1972; Jethani et al., 1992). The presence of these compounds promotes the HNO<sub>2(aq)</sub> and HNO<sub>3(aq)</sub> formation in water and influences the equilibria in the gas-phase. Due to its scarce solubility in water or into more alkaline solutions, NO<sub>(g)</sub> can desorb and thus can be absorbed again or partially oxidized to NO<sub>2(g)</sub> in the gas-phase, producing HNO<sub>2(g)</sub>, and partly reacts forming the two intermediates, N<sub>2</sub>O<sub>3(g)</sub> and N<sub>2</sub>O<sub>4(g)</sub>, reiterating the reactive loop in liquid-film above described.

The absorption of NO<sub>x</sub> in water is particularly influenced by the kinetic of NO<sub>(g)</sub> oxidation into NO<sub>2(g)</sub>, which represents the slow step of the whole process (Miller, 1987; Thiemann, 2000). A rigorous equilibrium and kinetic model that describes the complex chemical and physical phenomena in the two phases for the absorption of NO<sub>x</sub> in water, containing the constants for phase and chemical equilibria and kinetic parameters, is reported in Flagiello (2020). In order to achieve a high removal efficiency, NO can be converted to NO<sub>2</sub> in liquid-phase by using strong oxidants, such as sodium chlorite (NaClO<sub>2</sub>). Chlorite ions is mainly consumed to oxidize NO<sub>(aq)</sub> into NO<sub>2(aq)</sub> and then in nitrates, while ClO<sub>2</sub><sup>-</sup> is reduced to chlorides. Recent reports (Deshwal and Lee, 2009; Park et al., 2015) suggest that the oxidation reaction pathways with NaClO<sub>2</sub> can be divided into two different reactive pathways, depending on whether the reaction occurs under acidic conditions or not. The mechanism of NO<sub>x</sub> absorption in NaClO<sub>2</sub> solutions could be studied by considering only the oxidation reaction pathway with chlorite due to the poor solubility of NO<sub>(g)</sub> and NO<sub>2(g)</sub> in water and the very slow related reaction pathway (see Figure 1).

The oxidation reactions for NO<sub>x</sub> absorption at pH > 7 (Basic Oxidation Mechanism, BOM) are reported below:



where the Eq. (4) is given by the sum of the Eqs. (2)-(3), and represents the overall reaction for NO<sub>2</sub> oxidation. Standard Gibbs free energies of all reactions show that NO<sub>x</sub> is spontaneously absorbed and oxidized to HNO<sub>3(aq)</sub>, as also confirmed in the studies of Chien et al. (2003). The addition and/or formation of acid (H<sub>3</sub>O<sup>+</sup>)

resulting from the *BOM* mechanism, could trigger a second oxidation pathway when the pH falls below 7 (Flagiello, 2020) and chlorite ions are converted into chlorine ( $\text{Cl}_{2(\text{aq})}$ ) and chlorine dioxide ( $\text{ClO}_{2(\text{aq})}$ ), which are stronger oxidants that are able to increase the oxidation rate of  $\text{NO}_x$ . The reactions of formation of secondary oxidants are reported in Flagiello et al. (2020a), together with the equilibrium constants experimentally retrieved. The mechanism under acidic conditions (Acidic Oxidation Mechanism, *AOM*) is shown below.



A rigorous equilibrium model, including the constants of oxidation reactions, is reported in Flagiello (2020).

### 3. Materials and Methods

#### 3.1 Materials

The simulated flue-gas was prepared by mixing  $\text{NO}$  at 2% v/v in  $\text{N}_2$  stored in high-pressure cylinders with compressed air at technical grade. The further mixing of  $\text{O}_2$  contents in air with  $\text{NO}$  stream allows obtaining  $\text{NO}_2$  in simulated flue-gas. The scrubbing liquid stream was prepared with a tap water at  $\text{pH} = 7.6$  and its chemical composition, obtained by ionic chromatography method, is reported in Flagiello et al. (2018a). Sodium chlorite ( $\text{NaClO}_2$ ) was available at technical grade equal to 80% (w/w). The addition of sodium chlorite increased the pH value of the scrubbing solutions, which is equal to 8.96 and 9.40 for  $\text{NaClO}_2$  at 0.5% (w/w) and 1% (w/w), respectively.

#### 3.2 Experimental set-up

The flowsheet of the experimental set-up, inclusive of all the column equipment and measuring and analytical instruments, is shown in Figure 2.

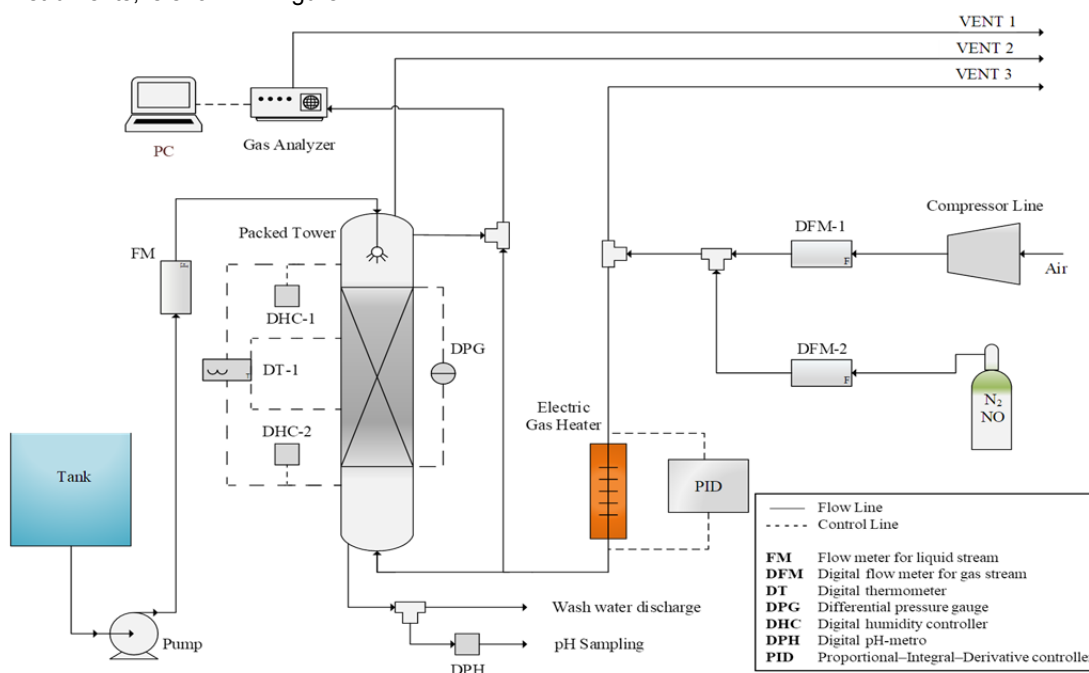


Figure 2: Flowsheet of the experimental set-up (Flagiello et al., 2020b)

The experiments were performed in a Plexiglas column operating at 1 bar, with a DN 100 and a packing height of 0.892 m using Mellapak 250.X packing. Mellapak 250.X modules are made in Hastelloy C-22 alloy to prevent acid corrosion; other geometric and physical characteristics are reported in Flagiello et al. (2018b; 2020c). The feeding gas section was managed via digital flow meters by SMC Corporation (with accuracy of  $\pm 1\text{NL}/\text{min}$ ) and its temperature was set at  $60\text{ }^\circ\text{C}$  using an electric gas heater provided by Megaris srl (total power of 1 kW), which was connected to a Proportional-Integral-Derivative (PID) controller for temperature

setting at the bottom inlet of the column. The column is also equipped with a gas pressure drop meter with a differential pressure gauge (FLUKE Corporation, 922 model with accuracy of  $\pm 0.1$  mmH<sub>2</sub>O). Moreover, the gas temperature profile was measured with a digital thermometer (PCE T-390 model with accuracy  $\pm 0.1$  °C) and the relative humidity at top and bottom was determined using a digital humidity controller (HOBO® onset UX100-23 model, with accuracy of  $\pm 0.1\%$  of relative humidity).

The scrubbing liquid was fed at the top of the column by a Grundfos Lenntech centrifugal pump (total power 0.75 kW) and controlled with a Cryotek Engineering flow meter (with accuracy of  $\pm 5$  L/h). The pH and temperature of the feeding liquid were measured with a digital pH-meter (PCE-228 model, with accuracy of  $\pm 0.01$  of pH and  $\pm 0.01$  °C for temperature). The liquid was atomized in the column by a PNR® full cone nozzle (DAM 1212 B31 model) with a complete opening of the liquid jet of 45°, and a 90 mm height plastic foam demister was put at 15 mm from the nozzle at the top of the column to block the entrained liquid drops.

### 3.3 Methodology of running tests and instrumental analytics

The experimental runs were carried out by feeding the simulated flue-gas stream to the column with a constant flow rate of 32 m<sup>3</sup>/h corresponding to 1.15 m/s, which is the typical gas velocity in a de-SO<sub>x</sub> scrubber (Flagiello et al., 2019). The gas temperature and its relative humidity were set to 60 °C and 10 - 15%, respectively. The NO<sub>x</sub> fed composition was set to 1030 ppm<sub>v</sub> and checked by a dedicated gas analyser (Eco Physics CLD 62) using the pipe-line before the scrubber. The scrubbing liquid stream was sent in counter-current flow with the gas at different flow rates, from 40 to 130 L/h. The liquid temperature was set at 25 °C, while the NaClO<sub>2</sub> dosages ranged from 0 to 1% (w/w).

The NO<sub>x</sub> gas concentration at the outlet of the column was monitored by the Eco Physics CLD 62 gas analyzer (limit of device is 100 up to 10000 ppm<sub>v</sub>), which allows measuring both NO and total NO<sub>x</sub> concentration. A gas sampling system was installed upstream to the gas analyzer, consisting of a KNF diaphragm pump (NMP 830 HP model), a Key Instruments flow meter (2500 Series, up to 1 L/min) and a Bühler Technologies gas quencher (TC-Standard Series). The experimental NO<sub>x</sub> removal efficiency ( $\eta_{NO_x}$ ) was calculated by comparing the input and output NO<sub>x</sub> concentration, as by Eq. (9).

$$\eta_{NO_x} = \frac{NO_{x,in} - NO_{x,out}}{NO_{x,in}} \quad (9)$$

The wash water was collected at the bottom of the column and sent to a sampling point for further analysis, i.e. temperature and pH value by digital pH-meter (PCE-228 model).

## 4. Results and Discussions

Figure 3 shows the experimental removal efficiencies of total NO<sub>x</sub> (A) and the final wash water pH (B) as a function of the liquid-to-gas volumetric ratio (L/G), varied between 1.25 and 4.06 L/m<sup>3</sup>. The results are shown parametrically with NaClO<sub>2</sub> loading (0 - 1% w/w).

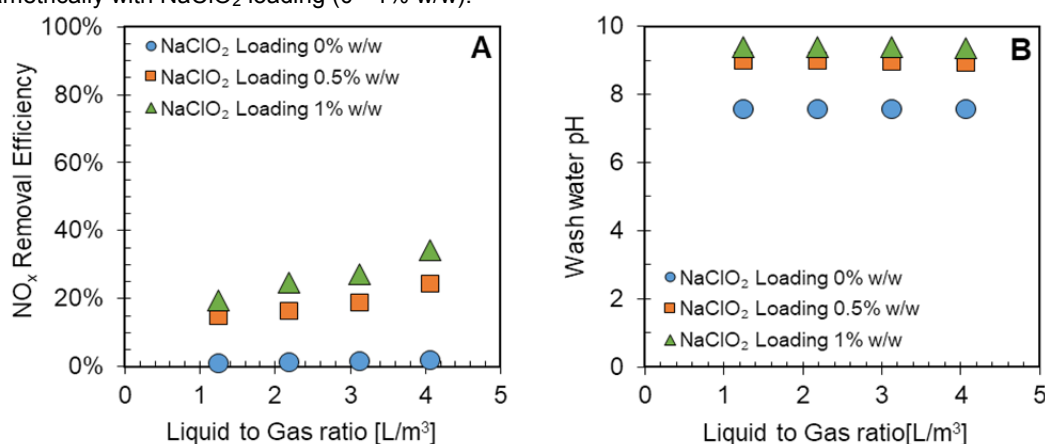


Figure 3: Experimental results of total NO<sub>x</sub> removal efficiency (A) and wash water pH (B) as a function of the Liquid-to-Gas ratio (L/G) and parametric with NaClO<sub>2</sub> loading in the scrubbing solution (from 0 to 1% w/w)

Figure 3A shows that the NO<sub>x</sub> removal efficiency in tap water (i.e. with 0% w/w NaClO<sub>2</sub> loading) is very low, up to 2%, consistently with the theory reported in the open literature and experiments with seawater by Flagiello et al. (2021). This was due to the low solubility of NO and NO<sub>2</sub> in water and to the very slow hydrolysis mechanisms (see Figure 1). On the contrary, the NO<sub>x</sub> removal efficiency increased up to 35% by increasing

the  $\text{NaClO}_2$  content. An appreciable influence of the liquid flow rate (or  $L/G$  ratios) was observed under these operating conditions, and the effects resulted more pronounced for  $\text{NaClO}_2$  at 1% w/w.

Figure 3B shows that the pH in the wash water solutions were negligibly affected by the  $L/G$  ratio. Besides, both the tap water and the  $\text{NaClO}_2$  solutions exhibited a final pH very close to the initial values (7.60, 8.94 and 9.40). While for the tap water no absorption takes place and, thus, the preservation of pH is expected, for  $\text{NaClO}_2$  solutions, this observation confirms that the reaction between chlorite and  $\text{NO}$  and  $\text{NO}_2$  in the aqueous phase occurred without altering the solution pH, according to the *BOM* mechanism reported in Eqs. (1)-(4). The results showed in Figures 3A-C were rearranged in Figure 4 to find a dependency between  $\text{NO}_x$  removal efficiency and the operating dosage ( $d_{op}$ ) defined as the ratio between the molar dosage of  $\text{ClO}_2^-$  in the scrubbing liquid and the  $\text{NO}_x$  in the fed flue-gas. A predictive equation was developed and showed in Figure 4.

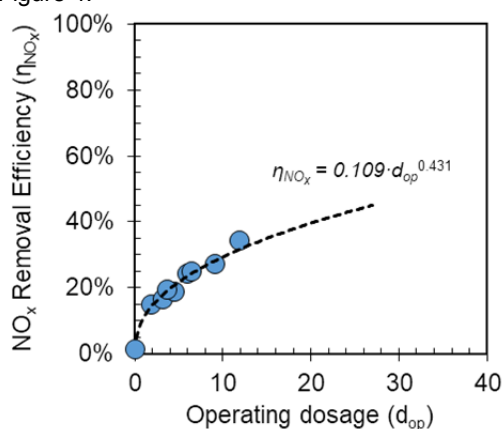


Figure 4: Experimental and modelling results of  $\text{NO}_x$  removal efficiency as a function of the operating dosage

Figure 4 shows that the  $\text{NO}_x$  removal efficiency increased with the operating dosage in the scrubbing solution. The data confirmed that  $\text{NO}_x$  oxidation was not strictly dependent on liquid flow rate but rather on the amount of  $\text{NaClO}_2$  used as compared to the  $\text{NO}_x$  in the gas fed. Figure 4 also shows that  $\text{NO}_x$  removal efficiency can be adequately described by a power law function in the tested range of  $\text{NaClO}_2$  dosages and, within certain validity limits, could allow to predict the performance of the process for higher operating dosages.

The maximum experimental removal achieved (35%) required a molar quantity of chlorite ions about 12 times greater than the  $\text{NO}_x$  one. As expected, to achieve higher  $\text{NO}_x$  removal values, the modelling equation predicts that an increasing excess of sodium chlorite must be added.

For a further reduction of emission limits as planned before and after 2030, the performance required for an existing de- $\text{NO}_x$  may be achieved using oxidative scrubbers as an end-of-pipe treatment. For example, considering that the further  $\text{NO}_x$  reduction must be equivalent to 60% of  $\text{NO}_x$  removal efficiency in the scrubber, a  $\text{NaClO}_2$  dosage about 50 times the  $\text{NO}_x$  molar fed is required. The large excess used could be a drawback for this operation, but a recirculation of a fraction of the wash water still containing the excess oxidant could make the process more attractive, reducing the costs.

## 5. Conclusions

This work aimed to evaluate the oxidative performances of sodium chlorite towards  $\text{NO}_x$ , to enhance the absorption of this compound, which is poorly soluble in water. The experiments were performed in a packed column operating with a model flue-gas at 1.15 m/s and 60 °C containing 1030 ppm<sub>v</sub> of  $\text{NO}_x$  and a scrubbing solution containing  $\text{NaClO}_2$ , with a dosage from 0 to 1% (w/w), at 25 °C.

The experimental results showed that for an oxidative scrubber the removal efficiencies increased with the addition of  $\text{NaClO}_2$  and by increasing the liquid flow rate. A maximum removal efficiency (35%) was observed for 1% (w/w)  $\text{NaClO}_2$  loading and a liquid-to-gas ratio equal to 4.06 L/m<sup>3</sup>, while a very lower efficiency (about 2%) using a tap water was obtained. The results also allowed to determine the main  $\text{NO}_x$  oxidation pathway, which resulted to be the mechanism under basic conditions (*BOM*, see Eqs. (1)-(4)); indeed, the wash water pH resulted to be higher than 7 in all the investigated conditions. The nitric acid produced during oxidation was unable to reduce pH due to the buffering effect of the tap water, and the second oxidation pathway under acidic conditions (*AOM*) did not occur (Eqs. (5)-(8)).

The operating molar dosage of  $\text{NaClO}_2$  that allowed to reach the maximum removal efficiency (35%) was equal to about 12 times the moles of  $\text{NO}_x$  in the gas fed. These results suggested that higher removals may be achieved by further increasing the  $\text{NaClO}_2$  loading in the scrubbing liquid. The experimental data also

confirmed that the  $\text{NO}_x$  removal efficiency can be expressed by a power law function with an exponent equal to 0.431 of the operating dosage,  $d_{op}$ .

This process could be suitable in the retrofitting of existing SNCR plants as an end-of-pipe process, where further efforts in terms of  $\text{NO}_x$  removal are required to comply with the more stringent recent regulations that will be in force with Directive (EU) 2016/2284. New generation of SCRs could also benefit for the integration of an oxidative scrubber, suitable for the abatement of a certain amount of  $\text{NO}_x$ , reducing CAPEX and O&M costs, and size of plant, as well as urea consumption and ammonia slip. Although a large excess of  $\text{NaClO}_2$  was necessary to achieve high levels of efficiency, as predicted by the retrieved model, the integration of a closed-loop scrubber system is recommended to optimize the oxidant consumption, hence reducing the costs of the chemicals. Further efforts are needed to investigate the oxidative scrubber operating in a closed-loop system to optimize the consumption of  $\text{NaClO}_2$  and the scrubber performance.

Future work will be also focused on the integration of a specific wash water treatment system after the oxidative scrubbing process and on the presence of  $\text{SO}_2$  in the simulated flue-gas or an artificial acidification of the oxidizing liquid in light of a potential improvement in the oxidative performances, as suggested by the literature.

### Acknowledgments

The Authors warmly acknowledge Eng. Maria Montieri for the support in the experimentation.

### References

- Brogren C., Karlsson H. T., Bjerle I., 1998, Absorption of NO in an aqueous solution of  $\text{NaClO}_2$ , *Chem. Eng. Technol.*, 21:1, 61-70.
- Chien T. W., Chu H., Hsueh H. T., 2003, Kinetic study on absorption of  $\text{SO}_2$  and  $\text{NO}_x$  with acidic  $\text{NaClO}_2$  solutions using the spraying column, *J. Environ. Eng.*, 129:11, 967-974.
- Deshwal B. R. and Lee H. K., 2009, Mass transfer in the absorption of  $\text{SO}_2$  and  $\text{NO}_x$  using aqueous euochlorine scrubbing solution, *Int. J. Environ. Sci.*, 21:2, 155-161.
- Flagiello D., Erto A., Lancia A., Di Natale F., 2018a, Experimental and modelling analysis of seawater scrubbers for sulphur dioxide removal from flue-gas, *Fuel*, 214, 254-263.
- Flagiello D., Di Natale F., Carotenuto C., Erto A., Lancia A., 2018b, Seawater Desulphurization of Simulated Flue Gas in Spray and Packed Columns: an Experimental and Modelling Comparison, *CET*, 69, 799-804.
- Flagiello D., Parisi A., Lancia A., Carotenuto C., Erto A., Di Natale F., 2019, Seawater desulphurization scrubbing in spray and packed columns for a 4.35 MW marine diesel engine, *ChERD*, 148, 56-67.
- Flagiello D., 2020, Enhanced seawater scrubbing for flue-gas cleaning, PhD Thesis, University of Naples Federico II, Naples, Italy.
- Flagiello D., Di Natale F., Erto A., Lancia A., 2020a, Wet oxidation scrubbing (WOS) for flue-gas desulphurization using sodium chlorite seawater solutions, *Fuel*, 277, 118055.
- Flagiello D., Erto A., Lancia A., Di Natale F., 2020b, Dataset of wet desulphurization scrubbing in a column packed with Mellapak 250.X, *Data in Brief*, 33, 106383.
- Flagiello D., Di Natale F., Lancia A., Erto A., 2020c, Characterization of mass transfer coefficients and pressure drops for packed towers with Mellapak 250.X, *ChERD*, 161, 340-356.
- Flagiello D., Di Natale F., Lancia A., Salo, K., 2021, Effect of Seawater Alkalinity on the Performances of a Marine Diesel Engine Desulphurization Scrubber, *CET*, 86.
- Gao F. et al., 2017, A review on selective catalytic reduction of  $\text{NO}_x$  by  $\text{NH}_3$  over Mn-based catalysts at low temperatures: catalysts, mechanisms, kinetics and DFT calculations. *Catalysts*, 7:7, 199.
- Hoftyzer P. J., Kwanten F. J. G., 1972, G. Nonhebel (Ed): *Gas Purification Processes for Air Pollution Control*, Butterworths, London, UK.
- Jethani K. R., Suchak N. J., Joshi J. B., 1992, Modeling and Simulation of a Spray Column for  $\text{NO}_x$  Absorption, *Comput. Chem. Eng.*, 16:1, 11-25.
- Miller D. N., 1987, Mass transfer in nitric acid absorption, *AIChE journal*, 33:8, 1351-1358.
- Muzio L. J., Quartucy G. C., Cichanowicz J. E., 2002, Overview and status of post-combustion  $\text{NO}_x$  control: SNCR, SCR and hybrid technologies, *Int. J. Environ. Pollut.*, 17:1-2, 4-30.
- Park H. W., Choi S., Park D. W., 2015, Simultaneous treatment of NO and  $\text{SO}_2$  with aqueous  $\text{NaClO}_2$  solution in a wet scrubber combined with a plasma electrostatic precipitator, *J. Hazard. Mater.*, 285, 117-126.
- Thiemann M., Scheibler E., Wiegand K. W., 2000, Nitric acid, nitrous acid, and nitrogen oxides, Chapter In: *Ullmann's encyclopedia of industrial chemistry*, Vol 26, Wiley-VCH, Weinheim, Germany, 177-225.
- Van Caneghem J. et al., 2016,  $\text{NO}_x$  reduction in waste incinerators by selective catalytic reduction (SCR) instead of selective non catalytic reduction (SNCR) compared from a life cycle perspective: a case study, *J. Clean. Prod.*, 112, 4452-4460.